Optical Transitions in Self- Organized CdSe Quantum Dots Thin Films

A. B. Sharma

Associate Professor, Nabira Mahavidyalaya, Katol-441302, Dist.-Nagpur, India.

Email: absktl@yahoo.com

Abstract

Highly luminescent CdSe nanocrystals have been assembled on glass/ ITO substrates using a wet synthesis route. The physical properties of the quantum dots have been investigated using optical absorption spectroscopy techniques. The optical transition energies have been determined for the lowest electron- hole pair states of CdSe quantum dots embedded in glass. The differential absorption spectra have been compared and general size dependence could be established. Considering theoretical models, the dominant features have been assigned to different transitions from the ground state to the one pair state.

Keywords: Quantum dots; CdSe

1. Introduction

Self –assembled CdSe nanostructures are promising material for display devices, sensors, data storage, optoelectronic devices etc. [1-4]. Electronic transitions in semiconductor quantum dots have been known to exhibit size depended behavior. Optical techniques have been extensively employed to probe the electronic state in quantum dots. The identification and assignment of the lowest electron-hole pair transitions in quantum dots is presently a subject of investigations [5-6]. Correct understanding of absorption and emission of quantum dots, would be very much helpful for developing tunable, highly efficient light emitting diodes and lasers.

2. Experimental Procedure:

The CdSe quantum dots have been assembled on glass/ITO substrates using a wet chemical synthesis route. In the synthesis of CdSe quantum dots, an aqueous medium containing Se and Cd as precursors were used. The Cd ion sources are obtained from cadmium chloride while the Se ions were sourced from stock solution of sodium seleno sulphite. The stock solution of sodium seleno sulphite was prepared using appropriate ratio of elemental selenium and anhydrous sodium sulphite in distilled water. The ratio of cadmium to selenium (3.18:1) was kept constant in the synthesis of all samples. The pH of the electrolyte

was maintained at 11 using ammonia solution. The surfactant used to control the size of quantum dots was mercaptoethanol. The variation in the mercaptoethanol to selenium ratio was from 0 to 2.42.

The HOMO- LUMO gap of the Q-CdSe film was determined by using optical absorption studies with the help of UV-Vis spectrophotometer (model UVPC 1601, Shimadzu Corporation, Japan) in the spectral range of 300- 800 nm using a spectral bandwidth of 2 nm at room temperature.

3. Results and Discussion:

The optical absorption spectra for four CdSe samples CK F (13.2 nm), CKV (3 nm), CKVI (2.8 nm) and CKVIII (1.9 nm) have been shown in fig. 1-4, respectively. The second order derivative spectra for each of the sample have also been shown in the insets of the corresponding figures. The absorption edges were identified with the help of the second order derivatives and have been summarized in table1. In each sample, the sharp rise in the absorption onsets correspond to the fundamental absorption edges which exhibit systematic blue shift with reduction in particle size. The quantum confinement of carrier within the quantum dots accounts for the observed blue shifts for the largest size CdSe nanoparticles (CKF), the absorption onset occurred at 680 nm (1.82 eV), which is slightly higher than the literature value of the bulk band gap of CdSe at room temperature 1.74 eV [Wikipedea, Trindade et al [2001]]. The Bohr exciton radius in CdSe is given by

$$a_{\mathrm{B}} = \frac{\varepsilon_o \varepsilon \lambda^2}{\pi m_o m^* e^2}$$

It can be calculated using ε = 10.6, to be 5.6 nm. Obviously the quantum size effects are likely to manifest in the size regime ≤ 5.6 nm. The largest shift corresponded to 2.84 eV for CdSe quantum dots of size 1.9 nm. Obviously the quantum size effects are likely to manifest in the size regime of ≤ 5.6 nm. The largest shift corresponded to 2.84 eV for CdSe quantum dots of size 1.9 nm.

Table 1 presents a summary of the ratio of surfactant to selenium ratio employed during quantum dot synthesis. The optical absorption data presented in fig 1 to 4, therefore, emphasize the effectiveness of mercaptoethanol in controlling the size of CdSe quantum dots.

In addition to the fundamental absorption onset, each of the CdSe samples exhibited a second absorption onset on the blue side. In order to understand the origin of the observed feature, we have to consider the band structure of CdSe.

Several reports have been published on the band structure calculation of the wurtzite phase of CdSe [7-10]. A typical band structure for cubic CdSe has been shown in figure 5 (Stukel et al [1969]). The valance band is contributed by the 4P orbital of Se. The valance band maxima are referred to as Γ_{15} at the Brillouin zone centre. The valence band, however, is six fold degenerate (including spin) at k=0. When the spin orbit coupling is strong, the degeneracy manifests as splitting of the Γ_{15} band into four-fold degenerate $P_{3/2}$ band (Γ_8) and a split off two-fold degenerate $P_{1/2}$ band (Γ_7). Note that the subscripts 3/2 or 1/2 refer to the total angular momentum J (=L+S). The conduction band made from the 5S electrons of cadmium is singly degenerate. Thus the cubic band structure at the zone centre, taking into account the spin orbit coupling can be schematically represented as shown in fig. 6.

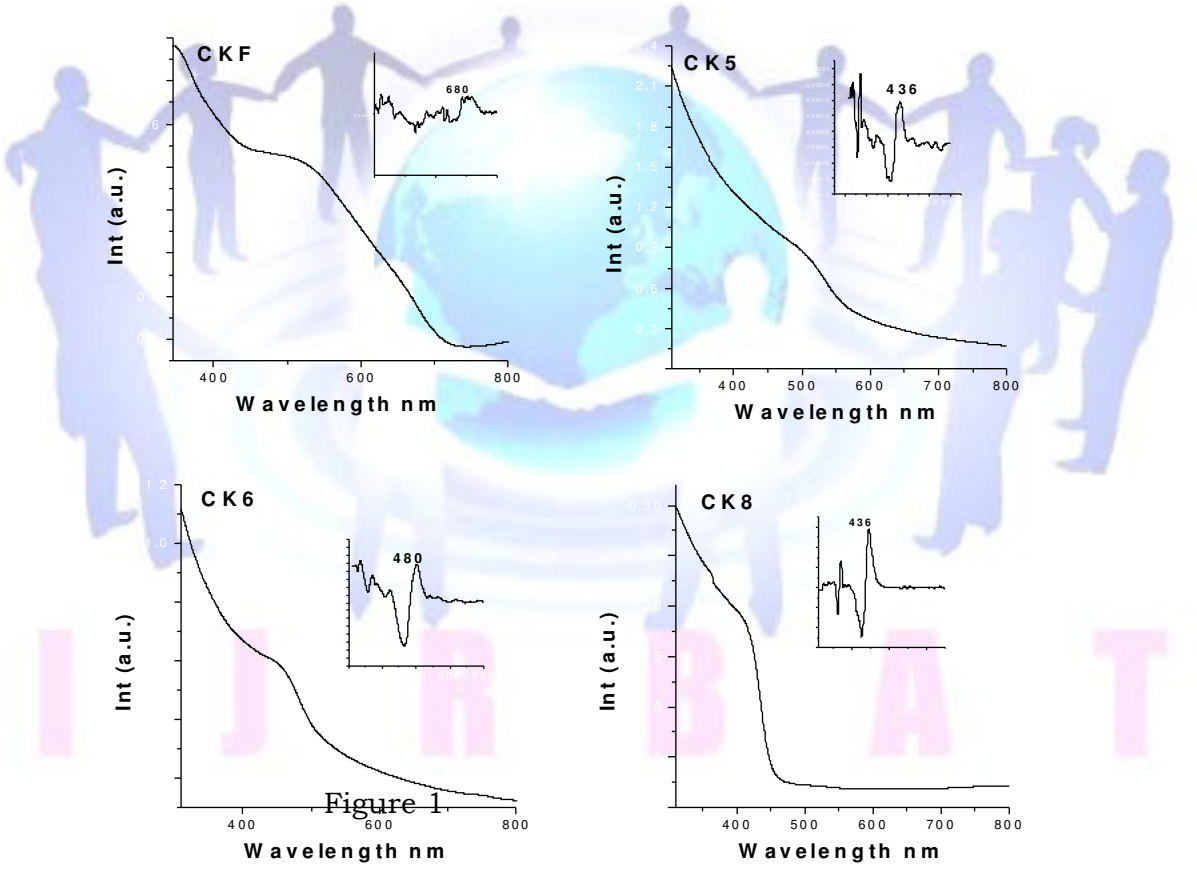

Figure 1

Figure 1-4: Optical absorption spectra of Q-CdSe nanocrystalline films (1) 13.2nm (2) 3 nm, (3) 2.8nm and (4) 1.9 nm.

In case of quantum dots, the band like levels transform into discrete energy states widely separated from each other. The optical transitions in CdSe quantum dots would thus involve the S level of the electron (conduction band) and three p-levels of the holes. This leads to simple terminology viz. $1S_e$ for electron levels in

any electron-hole pair formed. Thus Banin et al [11] labeled the transitions as $1S_{3/2}$-$1S_e$; $2S_{3/2}$-$1S_e$; $1S_{1/2}$-$1S_e$; $1P_{3/2}$-$1P_e$ etc.. It is thus obvious that the spin-orbit interaction leads to occurrence additional features in the absorption spectra of CdSe.

S.N.	Sample Name	Cappent/Se Ratio	Paticle Size (nm)	Spectral Position of fundamental absorption edge nm	eV
1	CKF	0	13	610	1.82
2	CKV	1:1	3.0	536	2.21
3	CKVI	1.23:1	2.8	480	2.58
4	CKVIII	2.42:1	1.9	436	2.84

Table 1: A summary of experimentally CdSe along the principal (From Stukel, et al [1969])

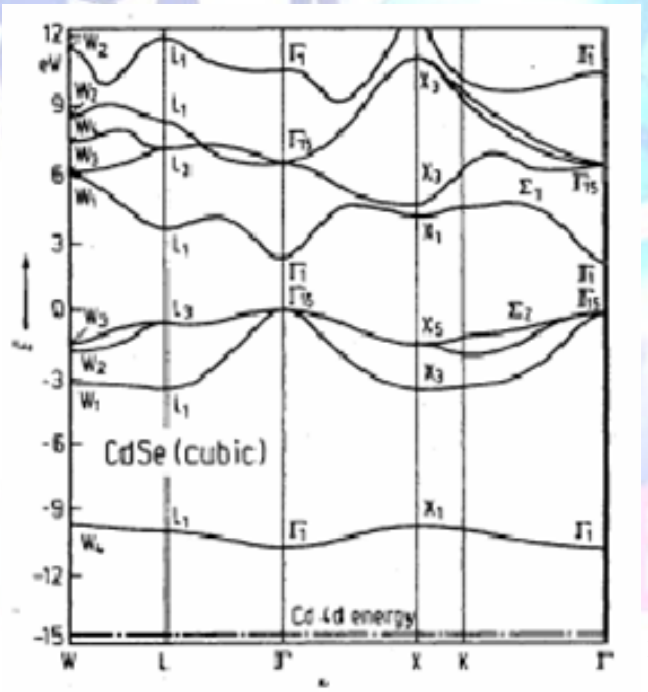

Figure 5 : Band diagram for bulk cubic determined optical absorption edges axis at Γ =0 for CdSe quantum dots.

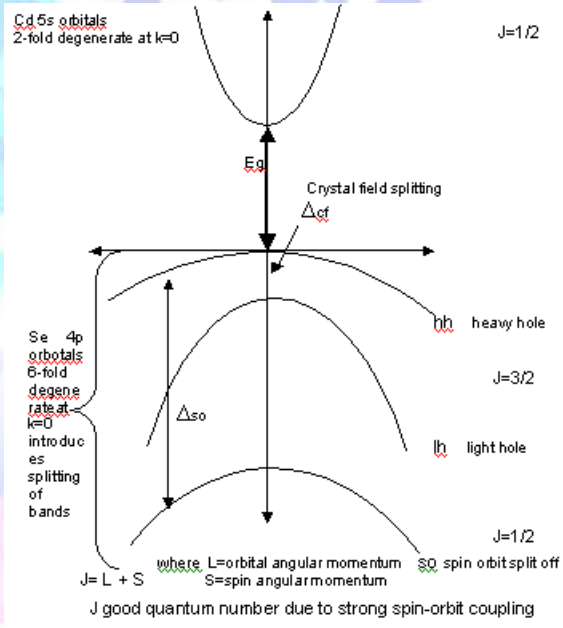

Figure 6 Schemtic band structure of cubic CdSe at Γ, including the spin orbit interaction

The experimentally determined positions of the absorption edges for all the four samples have been summarized in table 2, alongwith the corresponding labels. Note that the lowest transition labeled as $1S_{3/2}$-$1S_e$ corresponds to the fundamental absorption edge. The position of the next two higher transitions Viz. $2S_{3/2}$-$1S_e$ and $1S_{1/2}$-$1S_e$ have also been given. As expected the fundamental absorption edge

shifted to the blue side for decreasing particle size. The energy difference ΔE between the successively higher absorption edges Viz. a Viz. the fundamental absorption edge related transition ($1S_{3/2}$-$1S_e$) for all the four samples have also been calculated and summarized in table 2.

Table 2 : A summary of the observed absorption edges in CdSe. The lowest (fundamental) transition has been labelled as $1S_{3/2}$ $1S_e$.

SN	Transitions	CKF		Difference from lowest Exitation Side ΔE	CK-V		Difference from lowest ΔE	CK-VI		ΔE	CK-VIII		ΔE
		nm	eV	eV	nm	eV	eV	nm	eV	eV	nm	eV	eV
1	$1S_{3/2}$-$1S_e$	680	1.82	0.0	536	2.21	0.0	480	2.58	0.0	436	2.84	0.0
2	$2S_{3/2}$-$1S_e$	636	1.94	0.02	504	2.46	0.15	415	2.98	0.40	365	3.38	0.55
3	$1S_{1/2}$-$1S_e$	569	2.19	0.37	450	2.75	0.44	362	3.42	0.84	-	-	-

It is interesting to note that the energy separation ΔE increased with reduction in particle size. Size dependent hole spectrum in CdSe quantum dots have been theoretically investigated by several researchers [12-14]. The electron states for spherical quantum dots of zinc blende CdSe were obtained by neglecting the effect of the dielectric capping layer and treating the coulomb interaction between the electron-hole pairs as a perturbation. For hole states, the Luttinger Hamiltonian spherical approximation was used [15-17. The electrons were assumed to be confined within finite but very high potential barrier the holes were confined within an infinite potential barrier. With these basic assumptions the calculated differences ΔE between the lowest optical transitions was expected to increase for smaller quantum dots. While, this assumption is vindicated by our experimental results, exact composition with the theoretical data is unwarranted since the real quantum dots are always capped (and hence should experience a dielectric confinement also).

4. Conclusion:

The quantum dot boundary acts as a confinement barrier for the carrier wave functions, which remain delocalized inside the dot. The electronic excitations are also discretised as the size of the nanocrystal is reduced below the corresponding Bohr exaction radius. The Coulomb interaction and the mixing of states in CdSe quantum dots result in a strong change of the transitions from excited hole states to electron ground states. The electrons were assumed to be

confined within finite but very high potential barrier the holes were confined within an infinite potential barrier. The calculated differences ΔE between the lowest optical transitions increases for smaller quantum dots.

5. References:

1. S. Coe, W.K. Woo, M.G. Bawandi., V. Bulovic, *Nature (London).*, **420**, 800 (2002).
2. V.I. Klimov, A.A. Mikhaliovsky, S. Xu, A. Malko, J.A. Hollingsworth, C.A. Leatherdale, H.J. Eisler, M.G. Bawendi, *Science.*, **290**, 314 (2000).
3. M. Bruchez, Jr.M. Noronne, P. Gin, S. Weiss, A.P. Alivisotos, *Science.*, **281**,2013 (1998).
4. C.F. Hermandez, D.J. Suh, B. Kippelen, S.R. Marder, *Appl. Phys. Lett.*, **85**, 534 (2004).
5. D.J. Norris, A.Sacra, C.B.Murray and M.G.Bawendi, Phys. Rev. Lett. **72**, 2612 (1994).
6. A.I. Ekimov, F.Hache, M.C. Schanne- Klein, D. Richard, C.Flytzanis, I.A.Kudryatsev, T.V. Yazeva, A.V.Rodina and Al.L.Efros, J. Opt. Soc. Am. **B** 10 100 (1993).
7. Birman J. L.; Physical. Rev, **115**, 1493,(1959).
8. Bregstresser T. K., Cohen M.L.; Phys. Rev., **164**, 1069, (1967).
9. Stukel D.J., Euwema R. N., Collins T.C.; Phys.Rev., **179**, 74,(1969).
10. Sapra S., Sarma D.D., Viswanatha R.; Phys. Rev. B, **69**, 125304, (2004).
11. Banin U., Lee C.J., Guzelian A.A., Kadaronich A.V., Alivisatos A.P.; Superlatt. Microstruct, **22**, 559, (1997).
12. Norris D.J., Sacra A., Murray C.B., Bawendi M.G.; Phys.Rev.Lett., **72**, 2612(1994).
13. Efros Al. L, Rosen M, Kuno M; Phys. Rev. B, **54**, 4843,(1996).
14. Woggon U., Giessen H., Gindele F., Wind O., Flugel B., Pevgham B.N.; Phys. Rev. B, **54**, 17681, (1989).
15. Luttinger J.M; Phys. Rev., **102**, 1030, (1956).
16. Baldereschi A., Lipari N.C.;Phys. Rev. B, **3**, 439, (1971).
17. Lipari N.O., Baldereschi A.; Phys. Rev. B, **8**, 2697,(1973).